Journal of the Geological Society

U−Pb and Hf isotope data of detrital zircons from the Barberton Greenstone Belt: constraints on provenance and Archaean crustal evolution

Armin Zeh, Axel Gerdes and Christoph Heubeck

Email alerting service	click here to receive free e-mail alerts when new articles cite this article
Permission request	click here to seek permission to re-use all or part of this article
Subscribe	click here to subscribe to Journal of the Geological Society or the Lyell Collection

Notes

Lyell
Collection

U–Pb and Hf isotope data of detrital zircons from the Barberton Greenstone Belt: constraints on provenance and Archaean crustal evolution

ARMIN ZEH[1*], AXEL GERDES[1] & CHRISTOPH HEUBECK[2]

[1]*Institute of Geosciences, Goethe-University Frankfurt, Altenhöferallee 1, 60438 Frankfurt am Main, Germany*
[2]*Department of Geological Sciences, Freie Universität Berlin, Malteserstr. 74–100, 12249 Berlin, Germany*
*Corresponding author (e-mail: a.zeh@em.uni-frankfurt.de)

Abstract: Combined U–Pb and Hf isotope analyses of detrital zircons from the Fig Tree and Moodies Groups of the Barberton Greenstone Belt, South Africa, yield similar Hf isotope compositions and age populations, thus pointing to a similar provenance. Zircon populations of Fig Tree Group greywacke and Moodies Group quartzarenite are both dominated by age clusters at 3.53, 3.47, and 3.28 Ga, and a minor cluster at 3.36 Ga. The Moodies quartzarenite sample additionally contains a younger age population at 3.23–3.19 Ga. Hafnium isotope data indicate that the source area of both sediments was affected by new crust formation from depleted mantle sources at 3.53, 3.47, and perhaps at 3.36 Ga (εHf_t between −1.7 and +4.5), accompanied by partial reworking of an Eoarchaean crustal component as old as 3.75–3.95 Ga. In contrast, crustal reworking was the predominant process between 3.28 and 3.22 Ga (εHf_t between −6.0 and +0.9), probably related to subduction and collision of terranes along the Inyoka Fault system. The zircon U–Pb and Hf isotope datasets favour a southern provenance for the Fig Tree and Moodies sediments, comprising granitoids in the vicinity of the southern Barberton Greenstone Belt and in Swaziland. This finding is in contrast to the sedimentary record of the Moodies Group, which mostly suggests a northern and along-strike provenance. This discrepancy may be due to reworking of sediments during extensive syn- and postorogenic strike-slip faulting and high uplift or subsidence between 3.26 and 3.19 Ga.

Supplementary material: Results of *in situ* U–Pb and Lu–Hf isotope zircon analyses are available at www.geolsoc.org.uk/SUP18561.

The present-day geology of the Kaapvaal craton of southern Africa, one of the oldest continental nuclei worldwide, comprises several crustal blocks that are separated from each other by major lithospheric suture zones. These zones, which comprise the Inyoka Fault system of the Barberton Greenstone Belt and the Murchison–Tabazimbi Lineament of the Northern Kaapvaal Craton (Fig. 1), are interpreted as important terrane boundaries that formed during accretion of the Swaziland, Witwatersrand, and Pietersburg blocks (e.g. de Wit *et al.* 1992; Lowe & Byerly 1999; Poujol *et al.* 2003; Anhaeusser 2006; Schoene *et al.* 2009; Zeh *et al.* 2009). The Inyoka Fault system of the Barberton Greenstone Belt is considered to have originated from a *c.* 3.3–3.2 Ga subduction–accretion event that caused syntectonic magmatism, syn-contractional strike-slip basin development, and high-grade metamorphism (Kröner *et al.* 1991; de Wit *et al.* 1992; de Ronde & de Wit 1994; Kamo & Davis 1994; Lowe 1994; Lowe & Byerly 1999; de Ronde & Kamo 2000; Dziggel *et al.* 2002; Stevens *et al.* 2002; Diener *et al.* 2005; Moyen *et al.* 2006; Schoene *et al.* 2008, 2009; Zeh *et al.* 2009; Schoene & Bowring 2010), followed by transform boundary deformation that culminated in *c.* 3.1 Ga granitic magmatism and differential exhumation of mid-crustal rocks on extensionally reactivated faults (Westraat *et al.* 2005; Schoene & Bowring 2007, 2010; Schoene *et al.* 2008). The subduction–accretion event ended in the collision of two major terranes (or terrane collages), which are characterized by distinct granitoid intrusion ages and isotope patterns. The Barberton South Terrane (definition of Zeh *et al.* 2009), comprising the Stolzburg, Steynsdorp and Swaziland subterranes (including large parts of the Onverwacht Group and Ancient Gneiss Complex, Fig. 1), is made up of granitoids with ages of 3.66, 3.55, 3.45, 3.33 and 3.23 Ga (e.g. Compston & Kröner 1988; Armstrong *et al.* 1990;

Kröner *et al.* 1991; Kamo & Davis 1994; Kröner & Tegtmeyer 1994; Schoene & Bowring 2007, 2010; Schoene *et al.* 2008; Zeh *et al.* 2009, 2011), whereas granitoids of the Barberton North Terrane are younger than 3.30 Ga (e.g. Kamo & Davis 1994; Poujol *et al.* 2003; Schoene *et al.* 2008; Zeh *et al.* 2009). In addition, the *c.* 3.23 Ga granitoids of the Barberton South Terrane always show near-chondritic εHf_t and εNd_t, indicating intense crustal reworking (Schoene *et al.* 2009; Zeh *et al.* 2009, 2011) whereas those of the Barberton North Terrane (e.g. Kaap Valley and Nelshoogte Plutons) have superchondritic εHf_t and εNd_t values, indicating derivation from a relatively juvenile source at the same time (Schoene *et al.* 2009; Zeh *et al.* 2009). Because of these differences provenance studies using combined U–Pb and Lu–Hf isotope data of detrital zircon grains have a high potential to provide robust information on the source area of sediments, which were deposited on either side of the Inyoka Fault during the *c.* 3.3–3.2 Ga subduction–accretion phase (i.e. the Fig Tree and Moodies Group metasandstones). This approach has been shown to be useful to obtain detailed information not only about the timing of magmatic and metamorphic processes in the source area but also to distinguish between mantle- and crust-related magma sources, the maximum age of deposition, and post-depositional metamorphic alteration (e.g. Gerdes & Zeh 2006, 2009; Zeh *et al.* 2008; Kaur *et al.* 2011). Furthermore, combined U–Pb and Lu–Hf isotope data can provide valuable information about the early Earth's crust–mantle evolution prior to the stabilization of the oldest cratons, as Archaean sediments often contain material that is older than the underlying cratonic crust. This, for example, is well reflected by the finding of Hadean and Eoarchaean zircons in metasediments of the Jack Hills and the Limpopo Belt, respectively (e.g. Maas *et al.* 1992; Zeh *et al.* 2008).

On a regional scale, detrital zircon data contribute an independent dataset to traditional sedimentary provenance indicators such as palaeocurrents, stratigraphic thickness or lithological variations, or textural data. In the Barberton Greenstone Belt, such tests are particularly required because currently available sedimentary and geochronological data are largely inconclusive. A limited set of U–Pb zircon ages of 3.4–3.5 Ga from Moodies Group conglomerates suggests a southern provenance (e.g. from the Onverwacht Group and/or the Ancient Gneiss Complex of Swaziland; Tegtmeyer & Kröner 1987; Kröner & Compston 1988), whereas sedimentary, petrological and structural data instead indicate a significant input from the north (Heubeck & Lowe 1994*a*; Heubeck & Lowe 1999). To address this controversy, to constrain sedimentary provenance and to define crustal makeup of the source area, we obtained combined U–Pb and Lu–Hf isotope data from detrital zircons from a representative metamorphosed Fig Tree Group litharenite and a Moodies Group quartzarenite.

Geological setting and samples

The Fig Tree and Moodies Group form the uppermost units of the Barberton Supergroup, the stratigraphic fill of the Barberton Greenstone Belt. The Fig Tree Group overlies the Onverwacht Group mostly conformably and consists of a southern shallow-water facies and a northern deep-water facies, separated by the Inyoka Fault system (Eriksson 1980; de Wit 1982; Lamb & Paris 1988). North of the Inyoka Fault, the Fig Tree Group traditionally consists of three formations, which are (from base to top) the Sheba, Belvue Road and the Schoongezicht Formation (Reimer 1967; Condie *et al*. 1970). The Sheba Formation comprises 750–1200 m of turbiditic lithic greywackes and shales, the Belvue Road Formation 600–1150 m of shale, turbiditic siltstone and greywacke, cherts, and locally volcaniclastic rocks and altered komatiitic lavas capped by a black shale near the top, and the Schoongezicht

Formation, *c*. 550 m of dacitic volcanic rocks, coarse-grained felsic volcaniclastic sandstones, conglomeratic breccias, tuffs, mudstones and some shale. Reimer (1983) additionally differentiated the Ulundi Formation, a 25–30 m thick iron-rich shale and chert unit, and Köhler & Anhaeusser (2002) recognized the 700–3000 m thick Bien Venue Formation, which mainly consists of aluminous quartz–muscovite schists and is apparently restricted to the northeastern Barberton Greenstone Belt. The latter formation is derived from a sequence of quartz-phyric dacitic to rhyodacitic volcaniclastic protoliths, dated at *c*. 3.256–3.259 Ga (Kröner *et al*. 1991), associated with subordinate banded chert, phyllite and chlorite schist, and overlies sediments correlated with the Belvue Road Formation. It is in turn discordantly overlain by Moodies Group conglomerates and sandstones. Units assigned to the Fig Tree Group south of the Inyoka Fault include the Mapepe and Auber Villiers formations, which were deposited between 3259 and 3225 Ma, based on dating of dacitic tuffs and agglomerates (e.g. Kröner *et al*. 1991; Byerly *et al*. 1996; Lowe & Byerly 1999; Lowe & Nocita 1999). Zircons from dacitic tuffs and agglomerates from the stratigraphically lowest and uppermost parts of the Fig Tree Group north of the Inyoka Fault are dated at 3.259 ± 0.003 Ga and 3.225 ± 0.003 Ga, respectively (Kröner *et al*. 1991; Byerly *et al*. 1996); xenocrysts from these rocks yielded ages between 3.522 and 3.323 Ga. SHRIMP analyses of 14 zircons from a Fig Tree Group greywacke from Swaziland (south to the Inyoka Fault) gave uniform ages of *c*. 3455 Ma (Kröner & Compston 1988).

The Moodies Group is the uppermost lithostratigraphic unit of the Barberton Greenstone Belt, and mostly occupies large synclines. The greatest stratigraphic thicknesses, highest petrographic variability and most diverse sedimentary facies are preserved in the synclines north of the Inyoka Fault. Anhaeusser (1976) subdivided the Moodies Group in the Eureka Syncline into three formations, including (from base to top) the Clutha, Joe's Luck and Baviaanskop Formation. Each of these formations is defined as an upward-fining
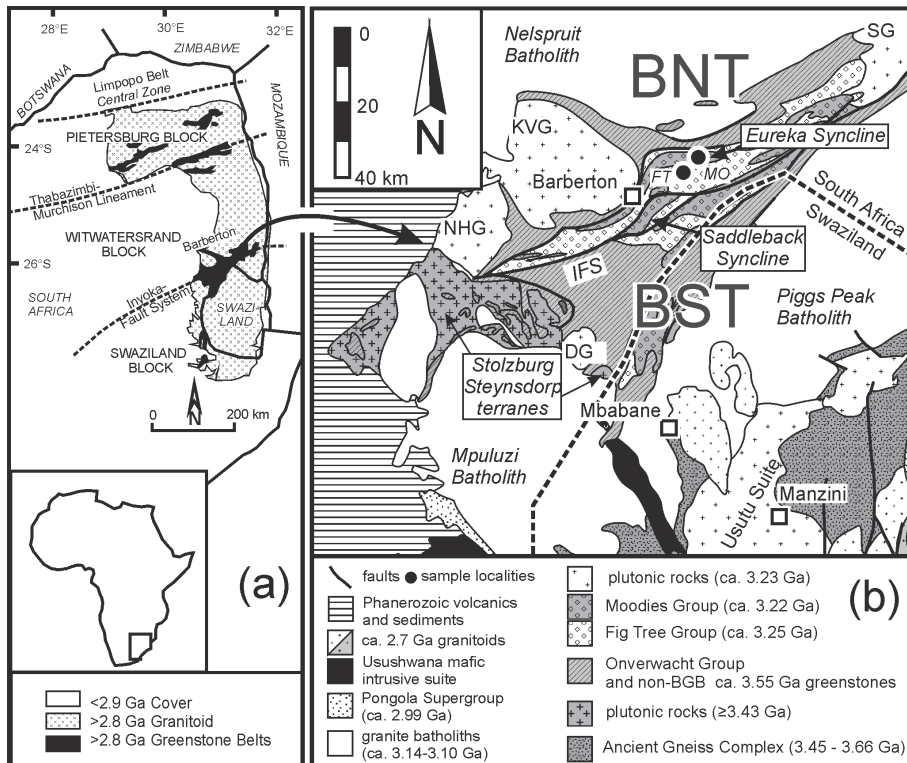

Fig. 1. (**a**) Archaean stratigraphic units of the eastern part of the Kaapvaal Craton in southern Africa. The crustal blocks are separated by major lineaments or fault systems. (**b**) Simplified geological map of the Barberton Greenstone Belt and the northern part of Swaziland (modified after Schoene *et al*. 2009). BNT, Barberton North Terrane; BST, Barberton South Terrane; KVG, Kaap Valley Granite; NHG, Nelshoogte Granite; DG, Dalmein Granite; SG, Salisbury Kop Granite; IFS, Inyoka Fault System.

cycle consisting of a coarse basal unit of conglomeratic quartzose sandstones, followed by a thick succession of finer-grained sandstones, siltstones and shales, and usually terminating with some jaspilitic banded iron formation. However, this first-order lithostratigraphic framework can only partially be correlated with the thicker stratigraphic column of Moodies strata in the Saddleback Syncline or with the more distal Moodies Hills Block and Stolzburg Syncline. Eriksson (1979), without defining a type location, recognized five major units (MD1–MD5) in the Eureka and Saddleback Synclines.

Moodies strata north of the Inyoka Fault record a range of terrestrial and shallow-marine environments, including alluvial, fluvial–deltaic, shoreline, tidal, and shallow–middle shelf deposits (Eriksson 1979, 1980; Heubeck & Lowe 1994a). They are up to 3000 m in thickness, extend over a strike length of >60 km and are correlatable to some degree through a few marker units within the dominantly sandy lithologies. In contrast, Moodies Group strata south of the Inyoka Fault are far thinner (not more than several hundred metres in thickness), lack marker horizons and do not contain K-feldspar. Heubeck & Lowe (1999) argued that Moodies strata on either side of the Inyoka Fault were deposited diachronously and in separate fault-bounded basins. Facies and petrographic trends have been investigated only in the thick and diverse stratigraphic columns north of the Inyoka Fault; there, they represent a gradual transgressive trend from alluvial to shelfal facies, accompanied by increasing compositional maturity in sandstones and conglomerates, overlain by a shallowing-upwards trend represented by alluvial fan-deltas and reflecting abrupt decrease in compositional maturity. Heubeck & Lowe (1994a) interpreted the former (Oosterbeek Petrofacies of Heubeck & Lowe 1999) as a passive-margin-related or rift-related sequence trend and the overlying section (Elephant's Head Petrofacies of Heubeck & Lowe 1999) as a response to syndepositional up-to-the-north faulting along the northern Barberton Greenstone Belt margin, incipient basin inversion and greenstone belt shortening.

The start of Moodies Group deposition is well constrained by age data from felsic and dacitic volcanic rocks of the Schoongezicht Formation at the top of the Fig Tree Group, conformably underlying the Moodies Group. These volcanic rocks yielded ages of 3.224 ± 0.006 Ga (Kröner & Todt 1988), 3.225 ± 0.003 Ga (Kröner et al. 1991), and 3.226 ± 0.001 Ga (Kamo & Davis 1994). In contrast, the end of Moodies deposition is less well constrained. The postkinematic, granitic Salisbury Kop Pluton of the northeastern Barberton Greenstone Belt unambiguously crosscuts the greenstone belt fold fabric, including tightly folded Moodies strata. It has been dated at 3.079 ± 0.016 Ga (Heubeck et al. 1993), 3.109 +0.010/−0.008 Ga (Kamo & Davis 1994), and 3.100 ± 0.014 Ga (Zeh et al. 2009). Also, deformed Moodies strata were magnetically overprinted by the Kaap Valley Pluton at 3.214 ± 0.004 Ga, which is the Ar–Ar hornblende cooling age of the Kaap Valley Pluton (Layer et al. 1996). Single-grain zircon ages from thin felsic ash units within the upper Moodies Group in the Saddleback Syncline have yielded ages of 3231 ± 6 Ma (Heubeck et al. 2010).

Granitoid pebbles from the Moodies basal conglomerate of the Eureka Syncline yield a complex spectrum. Pebbles dated by Tegtmeyer & Kröner (1987), Kröner & Compston (1988) and Sanchez-Garrido et al. (2011) yield ages of c. 3.57 and c. 3.47 Ga. In addition, Sanchez-Garrido et al. (2011) identified younger pebbles with ages between 3.30 and 3.21 Ga (three out of 14 clasts). Although pebbles with ages of 3.57 and 3.47 Ga clearly point to a southern source area, south of the Inyoka Fault system, the younger pebbles may be derived from magmatic rocks on either side of the Inyoka Fault. Thus the age pattern of the granitoid clasts in the basal member of the Moodies Group indicates mostly but not

necessarily exclusively a southern provenance, and thus appears to support the tectonic scenarios of Eriksson (1979, 1980) and Jackson et al. (1987). In contrast, stratigraphic data of Heubeck & Lowe (1994a) suggest significant transport of Moodies material from the north and along strike. In addition, Heubeck & Lowe (1999) argued that Moodies strata south of the Inyoka Fault system have a greatly reduced thickness and show a fundamentally different petrographic composition.

The depositional setting of the Moodies sediments was originally considered to be a foreland basin (e.g. Jackson et al. 1987; Eriksson 1980), including alluvial fans, braided streams, delta plains, shallow-water coastal systems and shelf facies (Eriksson 1980; Heubeck & Lowe 1994a, b). More differentiated assignments based on detailed field work (Heubeck & Lowe 1994a) suggested that the basal conglomerates and the overlying fluvial sandstones were derived from the north. Shoreline-parallel, NE- or SW-directed transport and extensive reworking dominated overlying deltaic, tidal and marine facies. Northerly derived, southward-thinning fan-delta conglomerate(s) over progressive unconformities in the Joe's Luck Formation of the Moodies Group are interpreted to mark the beginning of basin shortening (Heubeck & Lowe 1994b).

The samples used in this study were taken from the eastern Eureka Syncline at two roadcuts along the Sheba Mine access road. Sample FT is a coarse-grained greywacke from the Sheba Formation of the Fig Tree Group (25°42′765″S, 31°09′478″E; altitude 660 m); sample MO is a well-sorted, medium-grained, horizontally stratified and cross-bedded quartzarenite from unit MdS1 (Clutha Formation of Anhaeusser 1976) of the Moodies Group (25°41′429″S, 31°10′484″E; altitude 560 m).

Results of U–Th–Pb and Lu–Hf isotope analyses

Analyses of the U–Th–Pb and Lu–Hf isotope systems were carried out by laser ablation inductively coupled plasma mass spectrometry (LA-ICP-MS) at the Goethe University of Frankfurt, using the methods described by Gerdes & Zeh (2006, 2009), with some modifications. A Resolution M50 LR 193 nm Excimer (Resonetics)
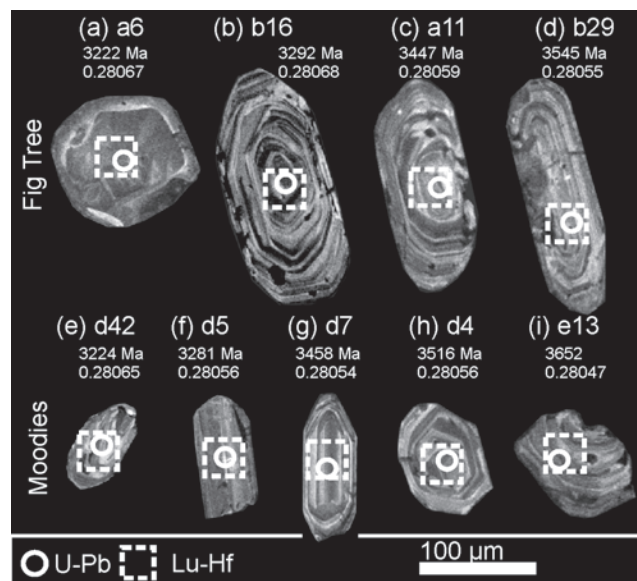

Fig. 2. CL images of detrital zircon grains from the Fig Tree Group greywacke and Moodies Group quartzarenite of the Eureka Syncline, with U–Pb and Lu–Hf laser spots.
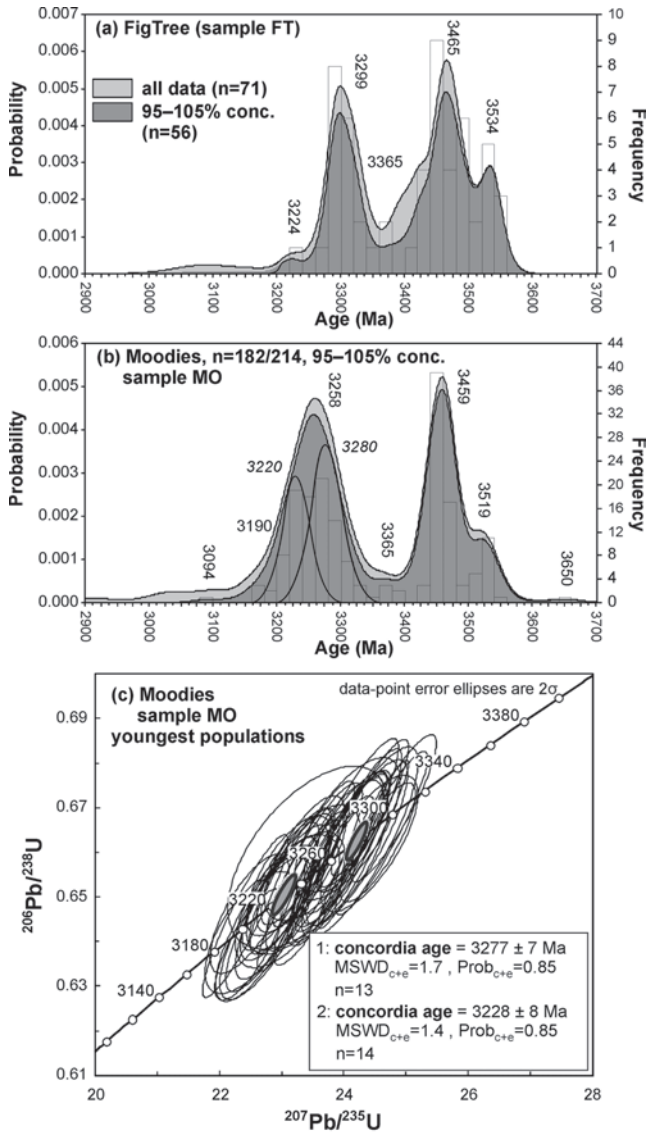
Fig. 3. Results of U–Pb analyses for samples FT (**a**) and MO (**b**, **c**) represented in probability/frequency v. age diagrams. Vertical numbers show ages of zircon populations obtained by the software AgeDisplay. Horizontal numbers mark age populations not recognized by AgeDisplay. (**c**) Concordia diagram showing U–Pb ages obtained by pooling the youngest major zircon population from sample MO into two groups.

laser system was used for sample ablation; U–Th–Pb and Lu–Hf isotope analyses were performed using a single-collector (Element 2) and multi-collector (Neptune) sector field ICP-MS system, respectively. A detailed description of the method is given in the Appendix. During this study we carried out U–Th–Pb analyses on 71 zircons of sample FT, and on 214 zircons of sample MO. Subsequently, Lu–Hf isotope analyses were obtained from the same zircons by placing the laser spots directly on top of or next to the U–Th–Pb spots. Laser spot locations were selected on the basis of the internal structures of the grains as seen in cathodoluminescence (CL) images of the mounted and polished grains (Fig. 2). The CL images show oscillatory zoning for most zircon grains, typical for zircon growth in igneous rocks (Fig. 2); however, some zircons show core–rim relationships. For this study, only zircon cores were
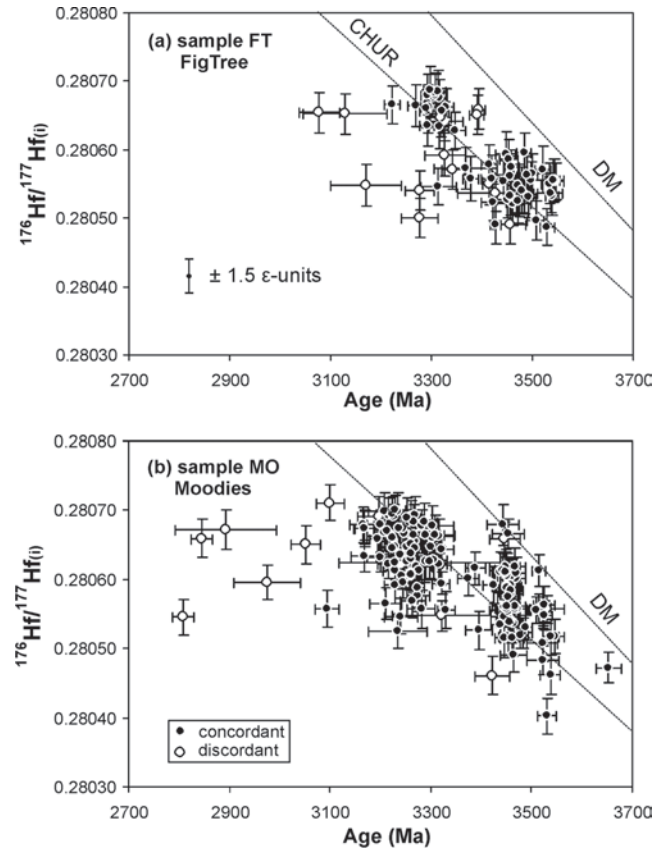

Fig. 4. $^{176}Hf/^{177}Hf$ v. Pb–Pb age diagram showing the results of combined U–Pb and Hf isotope analyses, for concordant and discordant analyses of sample FT (**a**) and sample MO (**b**). CHUR, chondritic uniform reservoir; DM, depleted mantle.

analysed. The $^{206}Pb/^{207}Pb$ age uncertainty of the single analyses is commonly less than ±0.02 Ga (2SD). Age spectra (Fig. 3) were plotted using the software AgeDisplay (Sircombe 2004) and include $^{206}Pb/^{207}Pb$ ages of all zircon analyses with a concordance level between 95 and 105%.

The U–Pb isotope data obtained from zircons of both samples show overall similar bimodal age spectra with predominant age peaks at 3.46 and 3.29–3.26 Ga. Subordinate populations occur at 3.54–3.52 and 3.37 Ga, and a single zircon of sample MO yielded 3.65 Ga (Fig. 3a and b). The youngest major age group of sample FT is relatively homogeneous, showing only small variations centred at 3.29 ± 0.02 Ga. Only one analysis in sample FT (grain a6) reveals a significantly younger age at 3.222 ± 0.017 Ga. In contrast, the youngest major age population of sample MO shows a much wider age variation (3.26 ± 0.05 Ga), as resolved by AgeDisplay, well outside the $^{206}Pb/^{207}Pb$ age error of the single analyses. This may indicate that the population comprises two distinct populations of 3.28 ± 0.02 and 3.22 ± 0.02 Ga (Fig. 3b). This is in agreement with calculated U–Pb concordia ages of 3.277 ± 0.007 Ga (*n* = 13) and 3.228 ± 0.008 Ga (*n* = 14), respectively (Fig. 3c). In addition, there are a few zircon analyses in sample MO that yielded significantly younger ages. Four analyses cluster at about 3.19 ± 0.02 Ga, and a single grain gave a concordia age of 3.095 ± 0.024 Ga (Fig. 3a).

Hafnium isotope data of the zircons from both samples show many similarities (Fig. 4). Zircons with ages >3.365 Ga have mostly superchondritic composition, whereas zircons with ages <3.33 Ga have subchondritic composition (Fig. 4). The Hf isotope
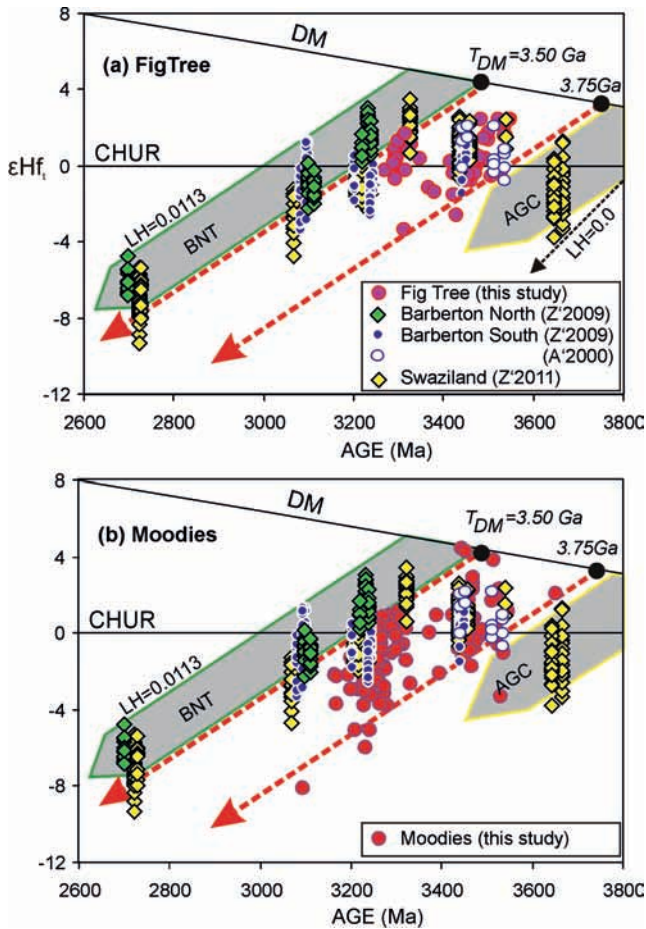
Fig. 5. Synopsis of εHf_t data of detrital zircon grains from the (**a**) Fig Tree Group and (**b**) Moodies Group (only concordant analyses) and from zircons of granitoids from the Barberton North and Barberton South terranes and Swaziland (data sources: A'2000, Amelin *et al.* 2000; Z'2009, Z'2011, Zeh *et al.* 2009, 2011). It should be noted that detrital zircons overlap well with data from the Barberton South Terrane and plot between the crustal evolution trends of the Ancient Gneiss Complex (AGC trend) and the Barberton North Terrane (BNT trend). LH = $^{176}Lu/^{177}Hf$. CHUR, chondritic uniform reservoir; DM, depleted mantle; T_{DM}, hafnium model ages.

variations extend to 8 epsilon units within the respective age population (Fig. 5). In general, εHf_t increases towards older ages, on average from −1.3 at 3.22 Ga to +1.6 at 3.53 Ga in sample FT, and from −1.8 at 3.23 Ga to +1.0 at 3.52 Ga in sample MO (Table 1).

Discussion

Provenance and depositional age

Age spectra and Hf isotope data provide evidence that both the Fig Tree Group greywacke (Sheba Formation) and Moodies Group quartzarenite (Clutha Formation) from the Eureka Syncline were derived from one or several similar source region(s) that experienced magmatic activity at 3.53 ± 0.2, 3.46 ± 0.2, 3.37 ± 0.2 and 3.29 ± 0.2 Ga (Fig. 3). The ages of the oldest detrital zircons from both samples (3.53 ± 0.2 and 3.46 ± 0.2 Ga) are in good agreement with intrusion ages of granitoids exposed to the south of the Inyoka Fault in the Barberton South Terrane (Fig. 1). The 3.53 Ga ages overlap with emplacement ages of the Steynsdorp tonalite, with tonalite wedges in the lower Onverwacht Group, with the age of Sandspruit Formation metavolcanic rocks, and with tonalite–trondhjemite–granodiorites (TTGs) of the Ancient Gneiss Complex (Compston & Kröner 1988; Kröner *et al.* 1989; Armstrong *et al.* 1990; Kamo & Davis 1994; Kröner & Tegtmeyer 1994; Amelin *et al.* 2000; Schoene *et al.* 2008; Zeh *et al.* 2009, 2011). In addition, they coincide with the oldest group of zircon ages from granophyric clasts from the basal Moodies conglomerate (Tegtmeyer & Kröner 1987; Kröner & Compston 1988; Sanchez-Garrido *et al.* 2011). Granitoids of the Ancient Gneiss Complex may be a potential source for the oldest zircon, with an age of 3.65 Ga, found in sample MO (Compston & Kröner 1988; Schoene *et al.* 2008; Zeh *et al.* 2011).

The abundant 3.46 Ga ages overlap with intrusion ages of plutonic rocks in the southwestern Barberton Greenstone Belt (e.g. Stolzburg and Theespruit Plutons), the intrusion age of the dacitic volcanic complexes at the top of the Kromberg Formation, and the Tsawela gneisses of Swaziland (Kröner *et al.* 1989; Armstrong *et al.* 1990; Kamo & Davis 1994; Byerly *et al.* 1996; Amelin *et al.* 2000; Schoene *et al.* 2008; Zeh *et al.* 2009, 2011). Because magmatic rocks with ages >3.4 Ga are unknown north of the Inyoka Fault, all aforementioned detrital zircons must have been supplied from a southern source.

Detrital zircons in both samples also record age populations of 3.29 ± 0.2 and 3.37 ± 0.2 Ga (Fig. 3). These ages overlap with those from metatuffs and ash beds of the upper Onverwacht Group

Table 1. *Hf isotope data of the age populations of sample FT and MO*

Age population (±30 Ma)	εHf_t (av.)	εHf_t (min.)	εHf_t (max.)	n
Sample FT				
3224	−1.3	−1.3	−	1
3299	−0.2	−5.9	+1.6	20
3365	+0.1	−1.8	+2.6	6
3465	+0.3	−2.0	+2.4	21
3534	+1.6	−0.5	+2.5	9
Sample MO				
3227	−1.8	−6.0	+0.3	34
3280	−0.9	−3.8	+1.1	37
3365	+0.5	0.0	+0.9	2
3459	+1.0	−1.7	+4.5	44
3519	+1.0	−3.3	+3.8	13
3650	+2.1	−	+2.1	1

(Kromberg Formation: 3.334 ± 0.006 Ga; Mendon Formation: 3.298 ± 0.006 Ga) and from a granitoid sample (3.323 ± 0.007 Ga) of the Ngwane gneiss of Swaziland (Byerly *et al.* 1996; Zeh *et al.* 2011). A similar age was also obtained from gneiss xenoliths in the Nelspruit 'granite' (Kamo & Davis 1994). These ages are not regionally specific: volcanic rocks of the Kromberg Formation occur only south of the Inyoka Fault, whereas Mendon volcanic rocks are exposed on either side of the Inyoka Fault, thus forming an overlap assemblage (Byerly *et al.* 1996). Thus, the 3.3 Ga zircons cannot serve well to distinguish a southern from a northern provenance.

The general absence of zircons with ages <3.265 Ga in the Fig Tree greywacke of the Sheba Formation indicates that the latter does not contain material from reworked 3.259 Ga dacites, which is widespread in the lower Fig Tree Group south of the Inyoka Fault (e.g. Kröner *et al.* 1991; Byerly *et al.* 1996). Sheba Formation greywackes are thus either older than 3.259 ± 0.003 Ga or had a different source. One or several restricted, well-defined source areas would be supported by the homogeneous age population of 3.45 Ga from a sample of southern-facies Fig Tree greywacke (Kröner & Compston 1988), whereas the northern facies sampled here is much more diverse. Considering the geological constraints and the obtained age spectra, we estimate the deposition age of Sheba greywacke at the sampled locality to be *c.* 3260 ± 10 Ma. However, a younger deposition age cannot completely be excluded, as a single grain of sample FT yielded a younger U–Pb age of 3.222 ± 0.017 Ga (grain a6). That single age, however, may reflect the timing of zircon alteration (see the irregular microstructure of grain a6 in Fig. 2a), accompanied by multiple (concordia-parallel) Pb loss. In any case, the obtained ages are in good agreement with the suggested depositional age of 3.359–3.225 Ga for the Fig Tree Group (Kröner *et al.* 1991; Byerly *et al.* 1996).

The Moodies Group sample contains, like sample FT, a major zircon age population at about 3.28 ± 0.02 Ga (Fig. 3), but also three younger age groups: abundant zircons at 3.228 ± 0.008 Ga, four grains at 3.19 ± 0.02 Ga, and a single grain at 3.095 ± 0.024 Ga. Apart from the youngest age, all other data are in good agreement with the suggested depositional age of 3.225–3.210 Ga for the Moodies Group (Heubeck *et al.* 2010). Sources of the youngest Moodies Group zircons (3.28–3.19 Ga) may include dacitic rocks of the lower Fig Tree Group south of the Inyoka Fault (Mapepe Formation: 3.259 ± 0.003 Ga), and the upper Fig Tree Group on either side of the Inyoka Fault (Schoongezicht Formation: 3.225 ± 0.003 Ga; Armstrong *et al.* 1990; Kröner *et al.* 1991; Kamo & Davis 1994; Byerly *et al.* 1996; de Ronde & Kamo 2000). Additional sources may have been the Kaap Valley and Nelshoogte Tonalites north of the Barberton Greenstone Belt (3227 ± 1 Ma; e.g. Kamo & Davis 1994), granitoids in the southwestern Barberton Greenstone Belt (Dalmein Pluton, 3216 ± 2 Ma; Kamo & Davis 1994) or abundant granites of the Usutu Suite in Swaziland (3236–3220 Ma; Schoene *et al.* 2008; Zeh *et al.* 2009, 2011; Schoene & Bowring 2010). This wide range of potential sources and regions is importantly limited by involving the Hf isotope data. These point to a southern provenance, as is supported by the overlap of the Hf isotope data of the detrital zircons with those of the 3.54–3.23 Ga granitoids of the Barberton South Terrane and from Swaziland (Amelin *et al.* 2000; Zeh *et al.* 2009, 2011). In contrast, granitoids of the Barberton North Terrane are more radiogenic and plot on a different trend (Fig. 5).

In summary, the combined U–Pb and Hf isotope datasets clearly show that zircons of the Fig Tree Group greywacke and Moodies Group quartzarenite samples were originally supplied from similar basement sources to the south of the Inyoka Fault system. Because both samples contain zircon populations with nearly identical Hf isotope data and similar age populations (at 3.53, 3.47. 3.36 and

3.28 Ga), sediments of both units either had access to the same source area or Moodies provenance included Fig Tree Group greywackes, regardless of their location. The common presence of unambiguous and specific Fig Tree clasts in Moodies conglomerates, including banded ferruginous chert and banded iron formation, shows that a variety of Fig Tree Group lithologies were indeed reworked during Moodies Group deposition but that only those most resistant to chemical weathering escaped mechanical disaggregation during transport, tidal reworking and intensive chemical weathering (Hessler & Lowe 2006). In fact, reworking of Fig Tree Group sediments in Moodies time would also explain the seeming contradiction of southern provenance indicated by zircon U–Pb–Hf isotope data and partial northern sources indicated by sedimentological data.

Archaean crustal evolution

The εHf_t values of the detrital zircons overlap well with those of granitoids from the Barberton South Terrane and Swaziland (Fig. 5), and nearly all data plot in a gap between the crustal evolution trend of the oldest granitoids from the Ancient Gneiss Complex of Swaziland (AGC trend in Fig. 5) and the granitoids from the Barberton North Terrane (BNT trend). Figure 5 also shows that the 3.53 and 3.47 Ga zircon populations show wide εHf_t variations between +4.5 and −1.7; that is, between values of depleted mantle and AGC crust. These values and variations indicates that new crust was formed from a depleted mantle source during both events, but also that crust–mantle mixing and crust reworking occurred in the hinterland at the same time. Hafnium model ages show that the reworked crust was on average not older than 3.75 Ga (see Fig. 5) except for one grain that yields a model age of 3.95 Ga (grain F52). The dataset also hints that new crust formation ceased after 3.45 Ga and that crustal reworking was the predominant process during 3.27 and 3.23 Ga magmatism (mostly subchondritic εHf_t), even though new crust formation between 3.45 and 3.23 Ga cannot completely be excluded. In fact, the observed εHf_t variations could be explained either by reworking of a pre-existing heterogeneous crust or by the mixing of crust–mantle matter. Whatever the cause, εHf_t values of the 3.23 Ga detrital zircons of sample MO are significantly lower than those of the 3.23 Ga TTGs of the Barberton North Terrane, which show superchondritic εHf_t at the same time (Fig. 5). This is an additional indication that the detrital zircons of the Moodies sample were not derived from the Barberton North Terrane but rather from south of the Inyoka Fault. In fact, the new dataset supports previous conclusions that ancient, more radiogenic crust of the Barberton South Terrane was reworked during terrane amalgamation at about 3.25 Ga whereas the Barberton North Terrane was affected by some new crust formation and/or by the reworking of a younger, less radiogenic crust at the same time (Schoene *et al.* 2008, 2009; Zeh *et al.* 2009, 2011).

Detrital zircons of both samples document Palaeoarchaean crust–mantle evolution but show no evidence of juvenile Eoarchaean or even Hadean crust in the source area. Thus, evidence for such an old hinterland in southern Africa is at present documented only by detrital zircons from *c.* 3.1 Ga sediments of the Limpopo Belt (Fig. 1), of which some zircons show U–Pb ages up to 3.9 Ga and hafnium model ages up to 4.45 Ga (Zeh *et al.* 2008).

Conclusions

Results of combined U–Pb and Lu–Hf isotope analyses on two samples show that Fig Tree Group greywacke and Moodies Group quartzarenite of the Barberton Greenstone Belt contain similar detrital zircon populations with ages at 3.53, 3.47, 3.36 and 3.28

Ga, and with overlapping Hf isotope compositions. The Moodies Group quartzarenite also contains a younger age population at 3.22–3.19 Ga. The source area of both sediments is characterized by new crust formation from depleted mantle sources at 3.53, 3.47, and perhaps at 3.36 Ga, accompanied by the partial reworking of older crust with Hf model ages between 3.95 and 3.75 Ga, and by significant crust reworking between 3.28 and 3.22 Ga. These data support the interpretation that zircons in both samples were originally dominantly derived from igneous rocks south of the Inyoka Fault, comprising the Stolzburg, Steynsdorp and Swaziland (sub) terranes. However, it remains unclear whether the detritus was continuously supplied from the same crustal source during deposition of both sediments or if Moodies Group quartzarenite was mainly derived from intensively reworked Fig Tree Group greywacke during extensive syn- and postorogenic strike-slip faulting and high uplift or subsidence between 3.26 and 3.19 Ga. In fact, reworking of Fig Tree sediments could solve the conundrum that some Moodies Group sediments reveal a southward directed transport, whereas detrital zircons require the opposite transport direction. A southern provenance for the Fig Tree and Moodies Group sediments also implies that Archaean basement rocks south of the Inyoka Fault were exposed at about 3.26 Ga, and that these basement rocks formed part of a morphological high (cordillera?) that perhaps existed until the end of terrane amalgamation at about 3.23 Ga. Thus, the results of this study demonstrate that combined U–Pb and Lu–Hf isotope data of detrital zircons not only set tight constraints on sediment provenances, but also can be useful for palaeolandscape reconstruction at the time of sediment deposition.

Appendix

U–Th–Pb isotope analyses

Uranium, thorium and lead isotopes were analysed using a ThermoScientific Element 2 sector field (SF)-ICP-MS system coupled to a Resolution M-50 (Resonetics) 193 nm ArF excimer laser (ComPexPro 102F, Coherent) system at Goethe-University Frankfurt. Data were acquired in time-resolved peak-jumping pulse-counting/analogue mode over 356 mass scans, with a 20 s background measurement followed by 21 s sample ablation. Laser spot size was 23 μm for unknowns and 33 μm for the standard zircons GJ1, 91500, and Plešovice. The sample surface was cleaned directly before each analysis by four pulses pre-ablation. Ablations were performed in a 0.6 l min^{-1} He stream, which was mixed directly after the ablation cell with 0.07 l min^{-1} N$_2$ and 0.68 l min^{-1} Ar before introduction into the Ar plasma of the SF-ICP-MS system. All gases had a purity of >99.999% and no homogenizer was used while mixing the gases to prevent smoothing of the signal. Signal was tuned for maximum sensitivity for Pb and U while keeping oxide production, monitored as ^{254}UO/^{238}U, below 0.5%. The sensitivity achieved was in the range of 9000–14000 c.p.s. μg g^{-1} for ^{238}U with a 23 μm spot size, at 5.5 Hz and 5–6 J cm^{-2} laser energy. The typical penetration depth was about 14–20 μm. The two-volume ablation cell (Laurin Technic, Australia) of the M50 allows detection and sequential sampling of heterogeneous grains (e.g. growth zones) during time-resolved data acquisition, owing to its quick response time of <1 s (time until maximum signal strength was achieved) and wash-out (<99.9% of previous signal) time of about 2 s. With a depth penetration of c. 0.7 μm s^{-1} and a 0.46 s integration time (four mass scans = 0.46 s = one integration) any significant variation of Pb/Pb and U/Pb on the micrometre scale is detectable. Raw data were corrected offline for background signal, common Pb, laser-induced elemental fractionation, instrumental mass discrimination, and time-dependent elemental fractionation

of Pb/U using an in-house MS Excel© spreadsheet program (Gerdes & Zeh 2006, 2009). A common-Pb correction based on the interference- and background-corrected ^{204}Pb signal and a model Pb composition (Stacey & Kramers 1975) was carried out. The ^{204}Pb content for each ratio was estimated by subtracting the average mass 204 signal, obtained during the 20 s baseline acquisition, which mostly results from ^{204}Hg in the carrier gas (c. 180–420 c.p.s.), from the mass 204 signal of the respective ratio. For the analysed sample the calculated common ^{206}Pb contents were mostly <1–2% of the total ^{206}Pb but in rare cases exceeded 20%. Laser-induced elemental fractionation and instrumental mass discrimination were corrected by normalization to the reference zircon GJ-1 (Jackson *et al.* 2004). Prior to this normalization, the inter-elemental fractionation (^{206}Pb*/^{238}U) during the 21 s of sample ablation was corrected for each analysis. The correction was done by applying a linear regression through all measured, common Pb corrected ratios, excluding the outliers (±2 standard deviation; 2SD), and using the intercept with the y-axis as the initial ratio. The total offset of the measured drift-corrected ^{206}Pb*/^{238}U ratio from the 'true' isotope dilution thermal ionization mass spectrometry (ID-TIMS) value (0.0983 ± 0.0004; ID-TIMS GUF value) of the analysed GJ-1 grain was around 10% and the drift over the day was less than 2%.

Reported uncertainties (2σ) of the ^{206}Pb/^{238}U ratio were propagated by quadratic addition of the external reproducibility (2SD) obtained from the standard zircon GJ-1 (n = 21; 2SD c. 1.3%) during the analytical session (c. 6 h) and the within-run precision of each analysis (2SE; standard error). for the ^{207}Pb/^{206}Pb ratio we used a ^{207}Pb signal-dependent uncertainty propagation (see Gerdes & Zeh 2009). The ^{207}Pb/^{235}U ratio is derived from the normalized and error propagated ^{207}Pb/^{206}Pb and ^{206}Pb*/^{238}U ratios assuming a ^{238}U/^{235}U natural abundance ratio of 137.88 and the uncertainty derived by quadratic addition of the propagated uncertainties of both ratios. The accuracy of the method was verified by analyses of reference zircon 91500 (1066.4 ± 5.8 Ma, MSWD of concordance and equivalence = 0.28, n = 8), and Plešovice (338.1 ± 2.3 Ma, MSWD$_{C+E}$ = 0.86, n = 7). The data were plotted using the software Isoplot (Ludwig 2001).

Lu–Hf isotope analyses

Hafnium isotope measurements were performed with a Thermo-Finnigan NEPTUNE multicollector ICP-MS system at GUF coupled to the same laser as described in the U–Pb method (Resolution M-50 193 nm ArF excimer laser). Rectangular laser spots with edge lengths of 43 μm were drilled with repetition rate of 5.5 Hz and an energy density of 6 J cm^{-2} during 55 s of data acquisition. All data were adjusted relative to the JMC475 ^{176}Hf/^{177}Hf ratio of 0.282160 and quoted uncertainties are quadratic additions of the within-run precision of each analysis and the reproducibility of JMC475 (2SD = 0.0033%, n = 8). Accuracy and external reproducibility of the method were verified by repeated analyses of reference zircon GJ-1, MudTank and Temora2, which yielded ^{176}Hf/^{177}Hf of 0.282012 ± 0.000024 (2SD, n = 26), 282494 ± 0.000026 (n = 12), and 0.282660 ± 0.000026 (n = 7), respectively. This is well within the range of solution mode data (Woodhead & Hergt 2005; Gerdes & Zeh 2006).

For calculation of the epsilon Hf (εHf$_t$) the chondritic uniform reservoir (CHUR) was used as recommended by Bouvier *et al.* (2008; ^{176}Lu/^{177}Hf = 0.0336 and ^{176}Hf/^{177}Hf = 0.282785), and a decay constant of 1.867 × 10^{-11} (average of Scherer *et al.* 2001; Söderlund *et al.* 2004). Initial ^{176}Hf/^{177}Hf$_t$ and εHf$_t$ for all analysed zircon domains were calculated using the apparent Pb–Pb ages obtained for the respective domains. Depleted mantle hafnium model ages (T$_{DM}$) were calculated using values for the depleted

mantle as suggested by Blichert-Toft & Puchtel (2010), with $^{176}Hf/^{177}Hf = 0.283294$ and $^{176}Lu/^{177}Hf = 0.03933$, corresponding to a straight depleted mantle (DM) evolution line with $\varepsilon Hf_{today} = +18$ and $\varepsilon Hf_{4.558\ Ga} = 0.0$. T_{DM} for all data were calculated by using the measured $^{176}Lu/^{177}Hf$ of each spot for the time since zircon crystallization, and a mean $^{176}Lu/^{177}Hf$ of 0.0113 for the Palaeoproterozoic–Archaean crust (mean of average continental crust as suggested by Taylor & McLennan (1985) and Wedepohl (1995)).

References

AMELIN, Y., LEE, D.-C. & HALLIDAY, A.N. 2000. Early–middle Archean crustal evolution deduced from Lu–Hf and U–Pb isotopic studies of single zircon grains. *Geochimica et Cosmochimica Acta*, **64**, 4205–4225.

ANHAEUSSER, C.R. 1976. The geology of the Sheba Hills area of the Barberton Mountain Land, South Africa, with particular reference to the Eureka Syncline. *Transactions of the Geological Society of South Africa*, **79**, 253–280.

ANHAEUSSER, C.R. 2006. A re-evaluation of Archean intracratonic terrane boundaries on the Kaapvaal Craton, South Africa: Collisional suture zones? *In*: REIMOLD, W.U. & GIBBSON, R. (eds) *Processes on the Early Earth*. Geological Society of America, Special Papers, **405**, 315–332.

ARMSTRONG, R.A., COMPSTON, W., DE WIT, M.J. & WILLIAMS, I.S. 1990. The stratigraphy of the 3.5–3.2 Ga Barberton Greenstone Belt revisited: A single zircon ion microprobe study. *Earth and Planetary Science Letters*, **101**, 90–106.

BLICHERT-TOFT, J. & PUCHTEL, I.S. 2010. Depleted mantle sources through time: Evidence from Lu–Hf and Sm–Nd isotope systematics of Archean komatiites. *Earth and Planetary Science Letters*, **297**, 598–606.

BOUVIER, A., VERVOORT, J.D. & PATCHETT, P.J. 2008. The Lu–Hf and Sm–Nd isotopic composition of CHUR: Constraints from unequilibrated chondrites and implications for the bulk composition of terrestrial planets. *Earth and Planetary Science Letters*, **273**, 48–57.

BYERLY, G.R., KRÖNER, A., LOWE, D.R., TODT, W. & WALSH, M.M. 1996. Prolonged magmatism and time constraints for sediment deposition in the early Archean Barberton greenstone belt: Evidence from the Upper Onverwacht and Fig Tree groups. *Precambrian Research*, **78**, 125–138.

COMPSTON, W. & KRÖNER, A. 1988. Multiple zircon growth within early Archean tonalitic gneiss from the Ancient Gneiss Complex, Swaziland. *Earth and Planetary Science Letters*, **87**, 13–28.

CONDIE, K.C., MACKE, J.E. & REIMER, T.O. 1970. Petrology and geochemistry of Early Precambrian greywacke from the Fig Tree Group, South Africa. *Geological Society of America Bulletin*, **81**, 2759–2776.

DE RONDE, C.E.J. & DE WIT, M.J. 1994. Tectonic history of the Barberton Greenstone belt, Southern Africa: 490 million years of Archean crustal evolution. *Tectonics*, **13**, 983–1005.

DE RONDE, C.E.J. & KAMO, S.L. 2000. An Archean arc–arc collision event: A short-lived (ca. 3 Myr) episode, Weltevreden area, Barberton greenstone belt, South Africa. *Journal of African Earth Sciences*, **30**, 219–248.

DE WIT, M.J. 1982. Gliding and overthrust nappe tectonics in the Barberton Greenstone Belt. *Journal of Structural Geology*, **4**, 117–136.

DE WIT, M.J., ROERING, C., *ET AL.* 1992. Formation of an Archaean continent. *Nature*, **357**, 553–562.

DIENER, J.F.A., STEVENS, G., KISTERS, A.F.M. & POUJOL, M. 2005. Metamorphism and exhumation of the basal parts of the Barberton greenstone belt, South Africa: Constraining the rates of Mesoarchean tectonism. *Precambrian Research*, **143**, 87–112.

DZIGGEL, A., STEVENS, G., POUJOL, M., ANHAEUSSER, C.R. & ARMSTRONG, R.A. 2002. Metamorphism of the granite–greenstone terrane south of the Barberton Greenstone Belt, South Africa: An insight into the tectono-thermal evolution of the 'lower' portions of the Onverwacht Group. *Precambrian Research*, **114**, 221–247.

ERIKSSON, K.A. 1979. Marginal marine depositional processes from the Archean Moodies Group, Barberton Mountain Land, South Africa: Evidence and significance. *Precambrian Research*, **8**, 53–182.

ERIKSSON, K.A. 1980. Transitional sedimentation styles in the Moodies and Fig Tree Groups, Barberton Mountain Land, South Africa: Evidence favouring an Archean continental margin. *Precambrian Research*, **12**, 141–160.

GERDES, A. & ZEH, A. 2006. Combined U–Pb and Hf isotope LA-(MC)ICP-MS analyses of detrital zircons: Comparison with SHRIMP and new constraints for the provenance and age of an Armorican metasediment in Central Germany. *Earth and Planetary Science Letters*, **249**, 47–61.

GERDES, A. & ZEH, A. 2009. Zircon formation versus zircon alteration—new insights from combined U–Pb and Lu–Hf in situ LA-ICP-MS analyses, and consequences for the interpretation of Archean zircon from the Central Zone of the Limpopo Belt. *Chemical Geology*, **261**, 230–243.

HESSLER, A.M. & LOWE, D.R. 2006. Weathering and sediment generation in the Archaean: An integrated study of the evolution of siliciclastic sedimentary rocks of the 3.2 Ga Moodies Group, Barberton greenstone belt, South Africa. *Precambrian Research*, **151**, 185–210.

HEUBECK, C. & LOWE, D.R. 1994a. Depositional and tectonic setting of the Archean Moodies Group, Barberton Greenstone Belt, South Africa. *Precambrian Research*, **68**, 257–290.

HEUBECK, C. & LOWE, D.R. 1994b. Late syndepositional deformation and detachment tectonics in the Barberton Greenstone Belt, South Africa. *Tectonics*, **13**, 1514–1536.

HEUBECK, C. & LOWE, D.R. 1999. Sedimentary petrology and provenance of the Archean Moodies Group, Barberton Greenstone Belt, South Africa. *In*: LOWE, D.R. & BYERLY, G.R. (eds) *Geology of the Barberton Greenstone Belt, South Africa*. Geological Society of America, Special Papers, **329**, 259–287.

HEUBECK, C., TOULKERIDIS, T., WENDT, J.I., KRÖNER, A. & LOWE, D.R. 1993. Timing of deformation of the Archaean Barberton greenstone belt, South Africa: Constraints from zircon dating of the Salisbury Kop pluton. *Journal of South African Geology*, **96**, 1–8.

HEUBECK, C., LOWE, D.R. & BYERLY, G.R. 2010. High but balanced sedimentation and subsidence rates (Moodies Group, Barberton Greenstone Belt), followed by basin collapse: Implication for Archaean tectonics. *Geophysical Research Abstracts*, **12**, Abstract 6260.

JACKSON, M.P.A., ERIKSSON, K.A. & HARRIS, C.W. 1987. Early Archean foredeep sedimentation related to crustal shortening: A reinterpretation of the Barberton sequence, southern Africa. *Tectonophysics*, **136**, 197–221.

JACKSON, S.E., PEARSON, N.J., GRIFFIN, W.L. & BELOUSOVA, E.A. 2004. The application of laser ablation-inductively coupled plasma-mass spectrometry to in situ U–Pb zircon geochronology. *Chemical Geology*, **211**, 47–69.

KAMO, S.L. & DAVIS, D.W. 1994. Reassessment of Archaean crustal development in the Barberton Mountain Land, South Africa, based on U–Pb dating. *Tectonics*, **13**, 167–192.

KAUR, P., ZEH, A., CHAUDHRI, N., GERDES, A. & OKRUSCH, M. 2011. Archaean to Palaeoproterozoic crustal evolution of the Aravalli orogen, NW India, and its hinterland: The U–Pb and Hf isotope record of detrital zircon. *Precambrian Research*, **187**, 155–167.

KÖHLER, E.A. & ANHAEUSSER, C.R. 2002. Geology and geodynamic setting of Archaean silicic metavolcaniclastic rocks of the Bien Venue Formation, Fig Tree Group, northeast Barberton greenstone belt, South Africa. *Precambrian Research*, **116**, 199–235.

KRÖNER, A. & COMPSTON, W. 1988. Ion microprobe ages of zircons from Early Archean pebbles and greywacke, Barberton Greenstone Belt, southern Africa. *Precambrian Research*, **38**, 367–380.

KRÖNER, A. & TEGTMEYER, A. 1994. Gneiss–greenstone relationships in the Ancient Gneiss Complex of southwestern Swaziland, southern Africa, and implications for early crustal evolution. *Precambrian Research*, **67**, 109–139.

KRÖNER, A. & TODT, W. 1988. Single zircon dating constraining the maximum age of the Barberton greenstone belt, southern Africa. *Journal of Geophysical Research*, **93**, 15329–15337.

KRÖNER, A., COMPSTON, W. & WILLIAMS, I.S. 1989. Growth of early Archean crust in the Ancient Gneiss Complex of Swaziland as revealed by single zircon dating. *Tectonophysics*, **161**, 271–298.

KRÖNER, A., BYERLY, G. & LOWE, D.R. 1991. Chronology of early Archean granite–greenstone evolution in the Barberton Mountain Land, South Africa, based on precise dating by single zircon evaporation. *Earth and Planetary Science Letters*, **103**, 41–54.

LAMB, S.H. & PARIS, I. 1988. Post-Onverwacht Group stratigraphy in the southeastern part of the Archean Barberton greenstone belt. *Journal of African Earth Sciences*, **7**, 285–306.

LAYER, P.W., KRÖNER, A. & MCWILLIAMS, M. 1996. An Archaean geomagnetic reversal in the Kaap Valley Pluton, South Africa. *Science*, **273**, 943–946.

LOWE, D.R. 1994. Accretionary history of the Archean Barberton greenstone belt (3.55–3.22 Ga), southern Africa. *Geology*, **22**, 1099–1102.

LOWE, D.R. & BYERLY, G.R. 1999. Stratigraphy of the west–central part of the Barberton Greenstone Belt, South Africa. *In*: LOWE, D.R. & BYERLY, G.R. (eds) *Geological Evolution of the Barberton Greenstone Belt, South Africa*. Geological Society of America, Special Papers, **329**, 1–36.

LOWE, D.R. & NOCITA, B.W. 1999. Foreland basin sedimentation in the Mapepe Formation, southern facies Fig Tree Group. *In*: LOWE, D.R. & BYERLY, G.R. (eds) *Geological Evolution of the Barberton Greenstone Belt, South Africa*. Geological Society of America, Special Papers, **329**, 233–258.

LUDWIG, K. 2001. *Isoplot/Ex, rev. 2.49. A Geochronological Toolkit for Microsoft Excel*. Berkeley Geochronology Center, Special Publications, 1a.

MAAS, R., KINNY, P.D., WILLIAMS, I.S., FROUDE, D.O. & COMPSTON, W. 1992. The Earth's earliest known crust: A geochronological and geochemical study of 3900–4200 Ma old zircons from Mt. Narryer and Jack Hills, Western Australia. *Geochimica et Cosmochimica Acta*, **56**, 1281–1300.

MOYEN, J.-F., STEVENS, G. & KISTERS, A.F.M. 2006. Record of mid-Archaean subduction from metamorphism in the Barberton terrain, South Africa. *Nature*, **442**, 559– 562.

POUJOL, M., ROBB, L.J., ANHAEUSSER, C.R. & GERICKE, B. 2003. A review of the geochronological constraints on the evolution of the Kaapvaal Craton, South Africa. *Precambrian Research*, **127**, 181–213.

REIMER, T.O. 1967. *Die Geologie der Stolzburg-Synklinale im Barberton Bergland (Transvaal, Südafrika)*. Diplomarbeit, Geologisch-Paläontologisches Institut, Universität Frankfurt.

REIMER, T.O. 1983. Pseudo-oolites in rocks of the Ulundi Formation, lower part of the Archaean Fig Tree Group (South Africa). *Precambrian Research*, **20**, 375–390.

SANCHEZ-GARRIDO, C.J.M.G., STEVENS, G., ARMSTRONG, R.A., MOYEN, J.-F., MARTIN, H. & DOUCELANCE, R. 2011. Diversity in Earth's early felsic crust: Paleoarchean peraluminous granites of the Barberton Greenstone Belt. *Geology*, **39**, 963–966.

SCHERER, E., MÜNKER, C. & MEZGER, K. 2001. Calibration of the lutetium–hafnium clock. *Science*, **293**, 683–687.

SCHOENE, B. & BOWRING, S.A. 2007. Determining accurate temperature–time paths in U–Pb thermochronology: An example from the SE Kaapvaal craton, southern Africa. *Geochimica et Cosmochimica Acta*, **71**, 165–185.

SCHOENE, B. & BOWRING, S.A. 2010. Rates and mechanisms of Mesoarchean magmatic arc construction, eastern Kaapvaal craton, Swaziland. *Geological Society of America Bulletin*, **122**, 408–429.

SCHOENE, B., DE WIT, M.J. & BOWRING, S.A. 2008. Mesoarchean assembly and stabilization of the eastern Kaapvaal craton: A structural–thermochronological perspective. *Tectonics*, **27**, TC5010, doi:10.1029/2008TC002267.

SCHOENE, B., DUDAS, F.O.L., BOWRING, S.A. & DE WIT, M. 2009. Sm–Nd isotopic mapping of lithospheric growth and stabilization in the eastern Kaapvaal craton. *Terra Nova*, **21**, 219–228.

SIRCOMBE, K.N. 2004. AgeDisplay: An EXCEL workbook to evaluate and display univariant geochronological data using binned frequency histograms and probability density distributions. *Computers and Geosciences*, **30**, 21–31.

SÖDERLUND, U., PATCHETT, J.P., VERVOORT, J.D. & ISACHSEN, C.E. 2004. The [176]Lu decay constant determined by Lu–Hf and U–Pb isotope systematics of Precambrian mafic intrusions. *Earth and Planetary Science Letters*, **219**, 311–324.

STACEY, J. & KRAMERS, J.D. 1975. Approximation of terrestrial lead isotope evolution by a two-stage model. *Earth and Planetary Science Letters*, **26**, 207–221.

STEVENS, G., DROOP, G.T.R., ARMSTRONG, R.A. & ANHAEUSSER, C.R. 2002. Amphibolite facies metamorphism in the Schapenburg schist belt: A record of the mid-crustal response to ~3.23 Ga terrane accretion in the Barberton greenstone belt. *South African Journal of Geology*, **105**, 271–284.

TAYLOR, S.R. & MCLENNAN, S.M. 1985. *The Continental Crust: Its Composition and Evolution*. Blackwell, Oxford.

TEGTMEYER, A. & KRÖNER, A. 1987. U–Pb zircon ages bearing on the nature of Early Archean Greenstone Belt evolution, Barberton Mountainland, southwestern Africa. *Precambrian Research*, **36**, 1–20.

WEDEPOHL, K.H. 1995. The compositions of the continental crust. *Geochimica et Cosmochimica Acta*, **59**, 1217–1232.

WESTRAAT, J.D., KISTERS, A.F.M., POUJOL, M. & STEVENS, G. 2005. Transcurrent shearing, granite sheeting and the incremental construction of the tabular 3.1 Ga Mpuluzi Batholith, Barberton granite–greenstone terrane, South Africa. *Journal of the Geological Society, London*, **162**, 373–388.

WOODHEAD, J.D. & HERGT, J.M. 2005. A preliminary appraisal of seven natural zircon reference materials for *in situ* Hf isotope determination. *Geostandards and Geoanalytical Research*, **29**, 183–195.

ZEH, A., GERDES, A., KLEMD, R. & BARTON, J.M., JR. 2008. U–Pb and Lu–Hf isotope record of detrital zircon grains from the Limpopo Belt—evidence for crustal recycling at the Hadean to early-Archean transition. *Geochimica et Cosmochimica Acta*, **72**, 5304–5329.

ZEH, A., GERDES, A. & BARTON, J.M., JR. 2009. Archean accretion and crustal evolution of the Kalahari Craton—the zircon age and Hf isotope record of granitic rocks from Barberton/Swaziland to the Francistown Arc. *Journal of Petrology*, **50**, 933–966.

ZEH, A., GERDES, A. & MILLONIG, L. 2011. Hafnium isotope record of the Ancient Gneiss Complex, Swaziland, southern Africa: Evidence for Archaean crust–mantle formation and crust reworking between 3.66 and 2.73 Ga. *Journal of the Geological Society, London*, **168**, 953–963.